

Supplementary Information for

Dirac charge dynamics in graphene by infrared spectroscopy

Z. Q. Li^{1*}, E. A. Henriksen², Z. Jiang^{2,3}, Z. Hao⁴, M. C. Martin⁴, P. Kim², H. L. Stormer^{2,5,6}, and D. N. Basov¹

¹ Department of Physics, University of California, San Diego, La Jolla, California 92093, USA

² Department of Physics, Columbia University, New York, New York 10027, USA

³ National High Magnetic Field Laboratory, Tallahassee, Florida 32310, USA

⁴ Advanced Light Source Division, Lawrence Berkeley National Laboratory, Berkeley, California 94720, USA

⁵ Department of Applied Physics and Applied Mathematics, Columbia University, New York, New York 10027, USA

⁶ Bell Labs, Alcatel-Lucent, Murray Hill, New Jersey 07974, USA

*e-mail: zhiqiang@physics.ucsd.edu

Spectral features in the raw reflectance/ transmission data and their connection to the broadening of the $2E_F$ threshold and residual absorption of graphene.

As discussed in the text, our study has uncovered an anomalous width of the $2E_F$ threshold and a strong residual absorption below $2E_F$ in the conductivity spectra of monolayer graphene. It is straightforward to relate both effects to features in the raw data. In Fig. S1 we compare the raw $R(V)/R(V_{CN})$ and $T(V)/T(V_{CN})$ spectra (blue curves) with similar spectra generated from a model $\sigma_i(\omega)$ spectrum for ideal graphene (black curves). The top panel details the input for these model calculations. In this panel we plot with the black line the conductivity of ideal graphene $\sigma_i(\omega)$ obtained using an analytical expression for the optical constants of graphene derived by Gusynin et al.¹:

$$\sigma_i(\Omega) = \frac{e^2 N_f}{2\pi^2 \hbar} \int_{-\infty}^{\infty} d\omega \frac{[n_F(\omega) - n_F(\omega')]}{\Omega} \frac{\pi}{4\omega\omega'} \left[\frac{2\Gamma(\omega)}{\Omega^2 + 4\Gamma^2(\omega)} - \frac{2\Gamma(\omega')}{(\omega + \omega')^2 + 4\Gamma^2(\omega')} \right] (|\omega| + |\omega'|)(\omega^2 + \omega'^2)$$

where $\omega' = \omega + \Omega$, $n_F(\omega) = \frac{1}{e^{(\omega - E_F)/T} + 1}$ is the Fermi distribution, $N_f = 2$ is the spin degeneracy, and $\Gamma(\omega)$ is an impurity scattering rate. A constant scattering rate Γ is used in the theoretical formula. In order to facilitate comparison with our mid-IR data, we have set the Fermi energy $2E_F = 5600 \text{ cm}^{-1}$. By setting the scattering rate to $\Gamma = 1 \text{ cm}^{-1}$ and temperature to $T = 45 \text{ K}$, we are able to model the threshold structure at $2E_F$ influenced by thermal broadening representing experimental conditions. We utilized the above equation in the interband region and in order to account for the free carrier response we augmented this result with the Drude Lorentzian $\sigma_l(\omega) = \sigma_{DC} / (1 + \omega^2 \tau^2)$, where $\sigma_{DC} = 100 * \pi e^2 / 2\hbar$ and a scattering rate $1/\tau = 30 \text{ cm}^{-1}$ is obtained from the transport data for our device. The

model $R(V)/R(V_{CN})$ and $T(V)/T(V_{CN})$ spectra were calculated based on the input $\sigma_1(\omega, V_{CN})$ spectrum in Fig. S1(a) using the procedure described in the Methods section. The dip-peak feature around 1000 cm^{-1} in all the experimental and model spectra in Fig. S1(b, c) is due to a phonon of SiO_2 . Vertical dashed lines in the plot show that the width $\delta 2E_F$ of the interband threshold in $\sigma_1(\omega)$ is determined by broadening of the high frequency edge in $T(V)/T(V_{CN})$. Furthermore, this connection was validated through calculations using different values of the phenomenological damping constant Γ . Thus with the guidance provided by modeling results in Fig.S-1 one can read the broadening of the $2E_F$ feature directly from the $T(V)/T(V_{CN})$ data and conclude that $\delta 2E_F \approx 1400 \text{ cm}^{-1}$ at all biases.

Model spectra are equally helpful for substantiating significant residual conductivity of graphene below the $2E_F$. For this purpose it is instructive to analyze the upper limit of the $T(V)/T(V_{CN})$ values at $\omega=2E_F$ corresponding to the maximum depletion of the conductivity under the applied bias. Our modeling shows that this upper limit is determined by the transmission of the graphene gated structure at the charge neutrality point $T(\omega, V_{CN})$ and the transmission of the Si substrate $T_{\text{sub}}(\omega)$ as $T(\omega, V_{CN})/T_{\text{sub}}(\omega)$, where $T_{\text{sub}}(\omega)$ is obtained from IR measurements and $T(\omega, V_{CN})$ is calculated from the multi-layer model using the theoretical universal conductivity $\sigma_1(\omega, V_{CN}) = \pi e^2/2h$ for graphene. Provided the residual conductivity is vanishingly small, the peak in $T(V)/T(V_{CN})$ spectra at $\omega=2E_F$ reaches the upper boundary. Under these latter conditions the amplitude of peaks in a series of spectra generated for different biases will trace the boundary of the shaded region in Fig.S-1(b). However, if the depletion of the conductivity at $\omega < 2E_F$ is incomplete, the residual absorption will reduce the amplitude of $T(V)/T(V_{CN})$ below the upper limit.. This is indeed the case for the experimental spectrum in Fig.S1-(b) taken at $V=71 \text{ V}$ and for the entire data set in Fig.1. Similarly, the amplitude of changes of reflectance is also reduced by the residual conductivity (Fig.S1-c). We note that deviations between experimental and model spectra is significant compared to the signal-to-noise of our measurements.

Here we stress that the magnitude of $\sigma_1(\omega, V)$ below the $2E_F$ threshold is sensitive to ambiguities with the choice of $\sigma_1(\omega, V_{CN})$. An assumption of the universal value for $\sigma_1(\omega, V_{CN})$ implies that the residual conductivity is as strong as $0.3 \cdot \pi e^2/2h$. Within limitations of our measurements we cannot unambiguously rule out $\sigma_1(\omega, V_{CN}) < \pi e^2/2h$ at energies below 4000 cm^{-1} and dependent on the input for $\sigma_1(\omega, V_{CN})$ the residual values at $\omega < 2E_F$ may significantly vary. Within these constraints, our data indicate either a breakdown of the universal conductivity $\sigma_1(\omega, V_{CN}) = \pi e^2/2h$ or significant residual conductivity below $2E_F$ at finite doping. Note that other experimental studies²⁻⁴ attest to the validity of $\sigma_1(\omega, V_{CN}) = \pi e^2/2h$ assumption in the entire mid-IR, which implies strong residual absorption below the $2E_F$ cut-off that is nearly independent of the applied voltage.

References:

1. Gusynin, V. P., Sharapov, S. G. & Carbotte, J. P. Unusual Microwave Response of Dirac Quasiparticles in Graphene. *Phys. Rev. Lett.* 96, 256802 (2006).
2. Mak, K.F. & Heinz, T. 2008 APS March Meeting, Abstract: L29.00006, unpublished
3. Nair, R. R. *et al.* Fine Structure Constant Defines Visual Transparency of Graphene. *Science* DOI: 10.1126/science.1156965 (2008).
4. Kuzmenko, A. B., van Heumen, E., Carbone, F. & van der Marel, D. Universal Optical Conductance of Graphite. *Phys. Rev. Lett.* 100, 117401 (2008).

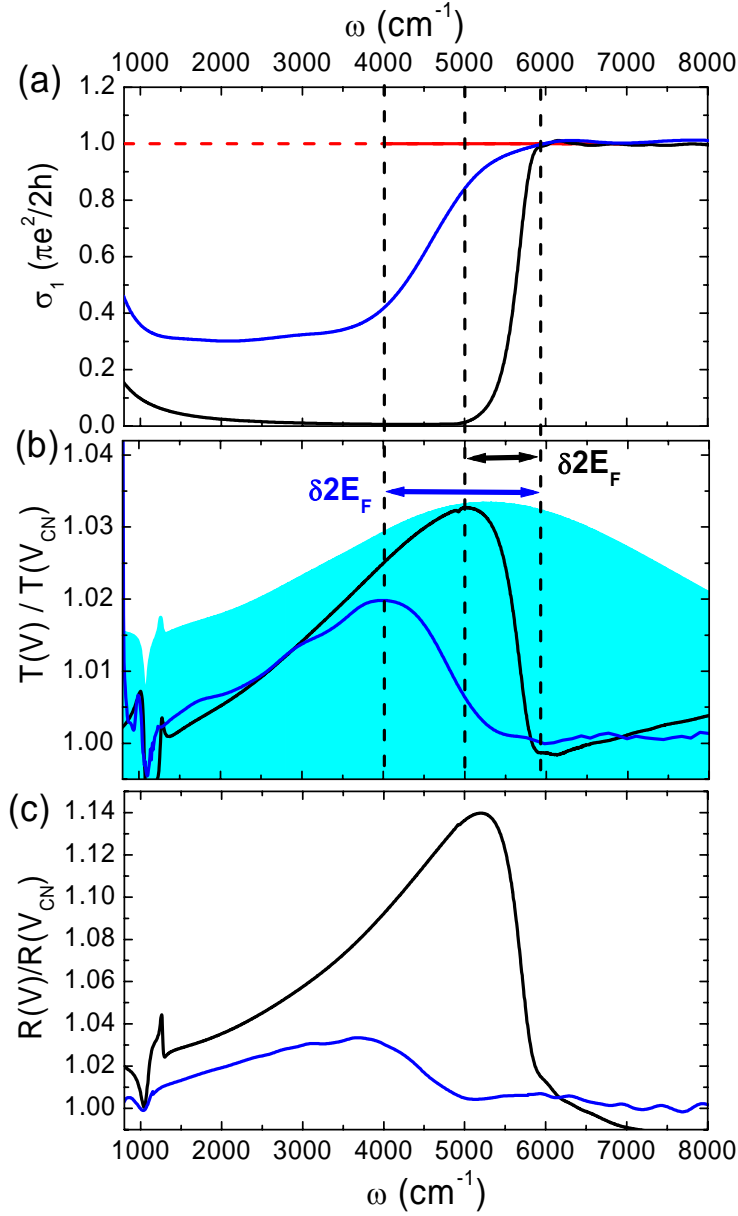


Figure S1: (a), the theoretical 2D optical conductivity $\sigma_1(\omega, V_{CN})$ at the charge neutrality point V_{CN} (red curve) and experimental $\sigma_1(\omega)$ spectrum at 71V (blue curve), together with a model $\sigma_1(\omega, 71 \text{ V})$ (black curve). The model spectrum reveals narrow width of the $2E_F$ threshold and negligible residual conductivity below $2E_F$. (b) and (c): experimental $R(V)/R(V_{CN})$ and $T(V)/T(V_{CN})$ spectra at 71V (blue spectra) and model data corresponding to the conductivity in (a) (black spectra). The upper boundary of the shaded region in (b) is the upper limit of $T(V)/T(V_{CN})$ values for different biases of our devices as described in the text. .